

Original Article

The value of susceptibility weighted magnetic resonance imaging in evaluation of patients with familial cerebral cavernous angioma

Haci Taner Bulut, Mehmet Akif Sarica, Ali Haydar Baykan

Department of Radiology, Medical Faculty of Adiyaman University, Adiyaman, Turkey

Received October 7, 2014; Accepted December 8, 2014; Epub December 15, 2014; Published December 30, 2014

Abstract: Objectives: We investigated the imaging features of Cavernous angioma (CA) lesions and the value of Susceptibility-weighted imaging (SWI) by comparing with T2*-weighted gradient echo (GRE) sequences in patients with familial CA disease. Material and methods: We retrospectively evaluated 19 familial CA patients (8 men, 11 women; mean age, 36 years). T1-weighted, T2-weighted, T2*-weighted GRE, and SWI sequences were performed to all patients. The numbers of CA lesions seen on T2*-weighted GRE and SWI sequences were analyzed. The correlations between the numbers of lesions on both sequences with age were evaluated. CA lesions were classified according to the classification of Zabramski et al. Results: The number of CA lesions was higher on SWI than T2*-weighted GRE significantly ($P < .001$). There was a significant strong correlation between the age of the patients and number of lesions in the cohort on T2*-weighted GRE ($r = 0.81$, $P < 0.001$) and SWI ($r = 0.85$, $P < 0.001$) sequences. Approximately 44% of the CA lesions which were detected only by SWI could not be categorized according to the classification of Zabramski et al. Conclusion: SWI can provide helpful additional information by determining the CA lesions more accurately than T2*-weighted GRE. Thus, routine clinical neuroimaging protocols should contain SWI to assess the true prevalence of lesions for optimal diagnosis and treatment. Moreover, this study show that the Zabramski classification is insufficient to identify all CA lesions, and a new type (type V) should be added to represent lesions that are seen on SWI but not on T2*-weighted GRE.

Keywords: Cavernous angioma, cavernoma, cavernous malformation, susceptibility-weighted imaging, T2*-weighted gradient echo

Introduction

Cavernous angiomas (CAs), also called cavernous malformations, cavernous hemangiomas, and cavernomas, account for 10%-15% of all intracranial vascular lesions [1]. The CA lesions consist as sporadic or familial forms. The familial form accounts for 10-30% of all cases and consists of both multifocal lesions and new lesions that develop during a normal lifetime [2-5]. According to series of autopsies, CAs occur in about 0.4% of normal population [6]. They are vascular lesions that are defined in histological terms by sinusoidal vascular spaces without cerebral parenchyma between them [6, 7]. CAs can cause various symptoms, such as headaches, seizures, hemorrhages, and focal neurological deficits. Nonetheless, some patients are completely asymptomatic [2-4, 7,

8]. The risk of hemorrhage and seizure precipitation for patients with cerebral CAs has been estimated at 3.1% and 2.4% per year, respectively [9].

Magnetic resonance imaging (MRI) is the best imaging technique of choice for diagnosis of cerebral CAs. MRI sequences have high sensitivity for detecting CAs [10]. Many CAs have a characteristic appearance on T2 weighted sequences, which includes a complicated central core and a peripheral rim of decreased signal intensity due to hemosiderin deposition in the surrounding parenchyma [8, 10, 11]. Until recently, T2*-weighted gradient echo (GRE) sequences admitted as the gold standard sequence in the evaluation of CA lesions in patients with familial forms of the disease [7, 10]. Susceptibility-weighted imaging (SWI) is a

relatively new high-spatial resolution, three-dimensional, GRE MRI sequence that utilizes the magnetic susceptibility differences of various tissues or substances, such as blood products, iron, and calcification [12, 13]. Recently, only two studies reported that SWI is more sensitive than T2*-weighted GRE sequences for evaluation of CA lesions [4, 5, 11]. Only de Souza et al. classified CA lesions according to the classification of Zabramski et al. [7]. They show that many of the CA lesions detected by SWI were not seen on T2*-weighted GRE sequences in patients with familial CAs (42.5% of total lesions). Nevertheless, they did not propose any modification for these lesions in Zabramski classification. Therefore, further studies are needed to add these lesions (CA lesions which are only detected by SWI) to Zabramski classification.

In the present study, we investigated the imaging features of CA lesions and the value of SWI by comparing with T2*-weighted GRE sequences in patients with the familial form of the disease. We hypothesized that SWI can provide additional helpful information to manage the diagnosis and treatment of familial form of CA patients.

Materials and methods

Subjects

In this retrospectively study, 19 familial CA patients were evaluated between November 2012 and April 2014. The cohort included 19 subjects (8 men and 11 women; mean age, 35.9 years; range, 15-57 years). Various neurological symptoms were recorded, including repeated history of headache (7 patients), seizure (7 patients), hemiparalysis (2 patients), hemianesthesia (1 patient), hearing loss (1 patient) and speech disfluency (1 patient). Only two patients were operated (one for intractable epilepsy and the other for hemorrhage) and their histological data were recorded. The institutional review board of our university hospital approved the study.

Magnetic resonance imaging method

A 1.5-T whole-body MRI system (Achieva; Philips Medical Systems, Best, The Netherlands) was used for all MRI examinations. T1-weighted, T2-weighted, T2*-weighted GRE,

and SWI sequences were performed in familial CA patients. Conventional spin-echo axial T1-weighted MRI was performed with a 23-cm viewing field and 5-mm thick sections with a 1-mm gap, matrix of 256×256, and TR/TE of 400/15 ms. Axial turbo spin echo T2-weighted images were obtained with a 23-cm viewing field, 5 mm-thick sections with a 1-mm gap, matrix of 384×512, and TR/TE of 4847/100 ms. Axial T2*-weighted GRE sequence parameters were as follows: repetition time/echo time, 699/23 ms; flip angle, 18; matrix, 256×256; viewing field, 23 cm; slice thickness, 5 mm; gap, 0 mm; and acquisition time, 3.49 min. For the SWI sequence, repetition time/echo time, 35/50 ms; flip angle, 15; matrix, 256×512; viewing field, 23 cm; slice thickness, 5 mm; gap, 0 mm; and acquisition time, 5.15 min. Two specialist radiologists independently counted the number of lesions on T2*-weighted GRE and SWI sequences randomly, and the final decision regarding the number of lesions was reached independently for all patients.

Zabramski et al. classified CA lesions according to their histological and MRI features [7]. The CA lesions were classified according to the classification of Zabramski et al. Type I lesions are characterized by hyperintense core on T1 and hyper- or hypointensity core on T2-weighted sequences. In type II lesions, CAs exhibit a core with reticulated mixed signal intensity on T2-weighted sequences and on T1-weighted images, with a well-circumscribed hypointense rim on T2-weighted sequences. Type III lesions show a iso- or hypointensity on T1-weighted sequence and a hypointensity on T2-weighted sequence as well as a rim that is hypointense on T2-weighted sequences. Type IV malformations are punctate hypointense lesions on T2*-weighted GRE MRI. The lesions seen only on SWI were considered independently of the Zabramski classification system [7]. This classification was performed by two readers who reached a final decision for all lesions independently.

Statistical methods

To assess interreader variability, Shrout and Fleiss intraclass correlation coefficients (ICCs) were used for the counted number of lesions [14]. ICCs were interpreted according to the criteria of Landis and Koch [15]. The following ICC categories were used for interpretation: 0.01-

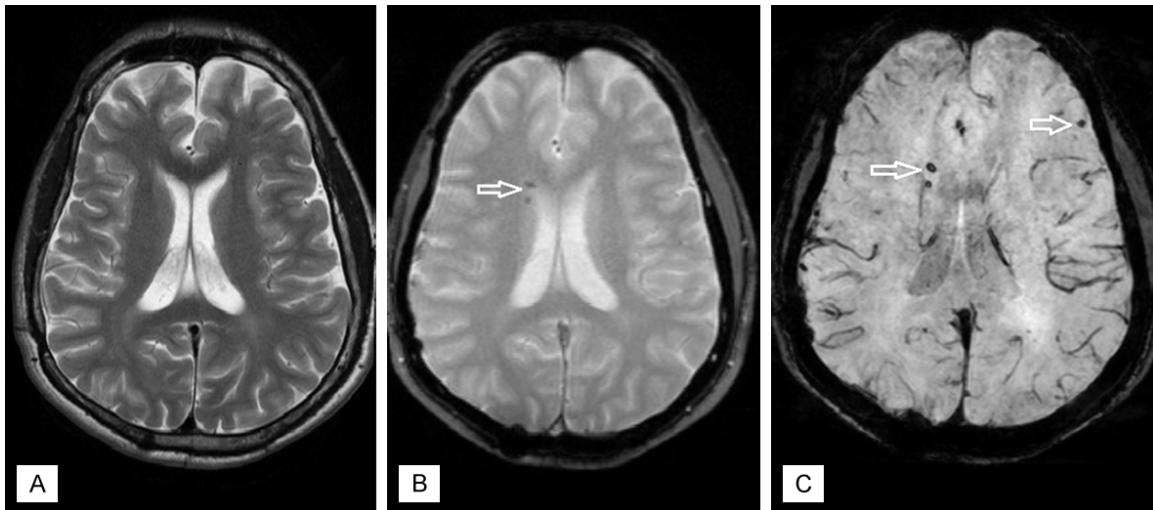


Figure 1. A. Axial T2-weighted image shows no significant abnormalities. B. Axial T2*-weighted GRE image shows a small two foci of low signal intensity (arrow) on the right subependymal region. C. SWI demonstrates the subependymal lesions (arrow), in addition, shows a left frontal lesion (arrow), which was not seen on T2*-weighted GRE image.

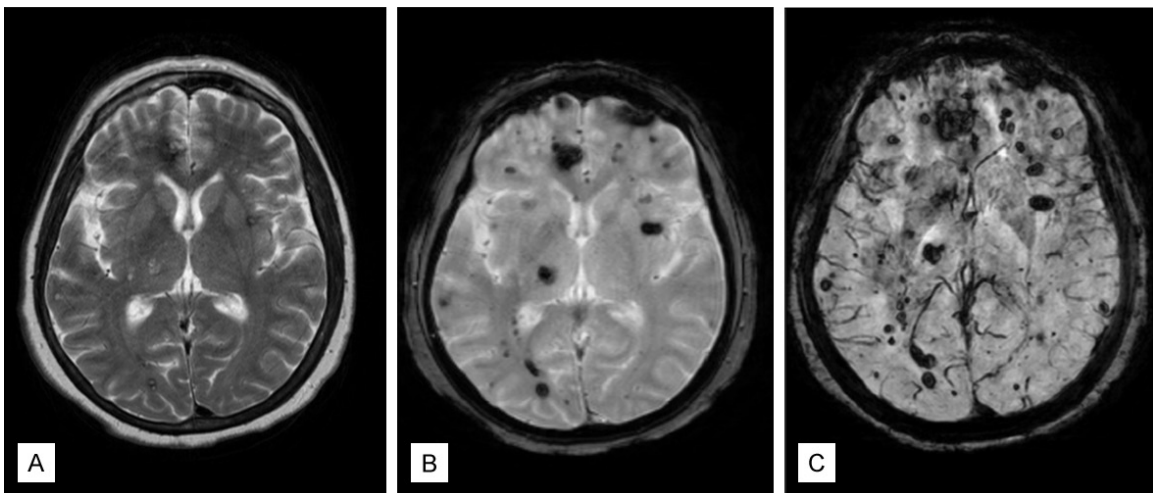


Figure 2. A. Axial T2-weighted image shows three focus of low signal intensity on the right frontal, occipital and left basal ganglia regions. B. T2*-weighted GRE image demonstrates multiple foci of low signal intensity on both cerebral hemisphere regions. C. SWI shows a higher number of lesions and confirms the presence of larger lesions, which are not seen on the T2*-weighted GRE image.

0.20 indicated slight agreement; 0.21-0.40 fair; 0.41-0.60 moderate; 0.61-0.80 substantial; 0.81-1.00 almost perfect. After ICC correlation, the average lesion counts determined by two readers were used for statistical analysis. The numbers of CA lesions seen on T2*-weighted GRE and SWI sequences were compared with the nonparametric Wilcoxon matched-pairs signed-rank test. The correlations between the numbers of lesions on both sequences with age were evaluated using the Spearman rank correlation coefficient. Possible

relationships between both sequences with age were analyzed using linear regression analysis. Statistical analyses were performed using Statistical Package for Social Sciences Version 17.0 (SPSS, Chicago, IL, USA), and $P < 0.01$ was taken to indicate significance.

Results

The first reader reported a mean of 30.7 lesions on T2*-weighted GRE (SD, 16.0; maximum, 52; minimum, 3) and 48.5 lesions on SWI (SD;

Value of SWI in cerebral cavernous angiomas

Table 1. Mean number of cavernous angiomas seen on T2*-weighted gradient echo and susceptibility-weighted imaging sequences

	Number of Lesions on T2-weighted GRE	Number of Lesions on SWI
First Reader ^a	30.7±16.04	48.5±22.92
Second Reader ^b	32.2±15.78	50.6±23.33
Mean of Readers ^c	31.4±15.19	49.5±22.82

GRE, gradient echo; SWI, susceptibility-weighted imaging. The number of lesions on T2*-weighted GRE and SWI sequences demonstrated a statistically significant difference (^a $P < .0001$, ^b $P < .0001$, ^c $P < .0001$).

Table 2. Intraclass correlation coefficients for interreader agreement in T2*-weighted Gradient Echo and Susceptibility-Weighted Imaging measurements

	T2*-weighted GRE	SWI
Patients with CA (n = 19)	0.942	0.898

GRE, gradient echo; SWI, susceptibility-weighted imaging; ICC, intraclass correlation coefficients, CA, cavernous angioma. The following ICC categories were used for interpretation: 0.01-0.20 = indicated slight; 0.21-0.40 = fair; 0.41-0.60 = moderate; 0.61-0.80 = substantial; 0.81-1.00 = almost perfect agreement.

22.9; maximum, 89; minimum, 4). The second reader found a mean of 32.2 lesions on T2*-weighted GRE (SD, 15.8; maximum, 56; minimum, 3) compared with 50.6 lesions on SWI (SD, 23.3; maximum, 97; minimum, 4) (**Table 1**). Illustrative cases are shown in **Figures 1, 2**. The number of CA lesions was higher on SWI than T2*-weighted GRE. Comparison of the numbers of lesions detected on SWI and on T2*-weighted GRE sequences indicated a statistically significant difference ($P < 0.0001$) (**Table 1**). The ICCs for the number of lesions counted on T2*-weighted GRE and SWI sequences ranged from 0.936 to 0.889 in patients with CAs (**Table 2**). According to the interpretation of Landis and Koch, this was an “almost perfect” interreader agreement for T2*-weighted GRE and SWI sequences [15]. In addition, there was a significant strong correlation between the age of the patients and number of lesions in the cohort on T2*-weighted GRE ($r = 0.81$, $P < 0.001$) and SWI ($r = 0.85$, $P < 0.001$) sequences. The correlation between the numbers of lesions on both sequences with age is shown in **Figure 3**.

According to the Zabramski classification, the first reader reported 28 (3.3%) type I lesions,

46 (5.5%) type II lesions, 56 (6.7%) type III lesions, and 338 (40.4%) type IV lesions. A substantial number of CA lesions ($n = 369$; 44.1%), which were seen only on the SWI sequence, could not be categorized according to the Zabramski classification. The second reader reported 31 (3.5%) type I lesions, 53 (5.9%) type II lesions, 62 (7.0%) type III lesions, and 356 (39.9%) type IV lesions. However, a substantial number of CA lesions ($n = 389$; 43.7%), which were seen only on the SWI sequence, could not be categorized according to the classification of Zabramski et al.

Discussion

MRI is the best imaging technique of choice for diagnosis of cerebral CAs [5, 8, 11, 16]. Because of differential magnetic susceptibility of blood products at different ages within the lesion, appearance of CAs may vary by MRI sequence. Clinically symptomatic CA lesions can be determined with close to 100% specificity and sensitivity, by T1- and T2-weighted sequences [5, 17]. Many CAs have a characteristic appearance on T2-weighted sequences, which includes a complicated central core and a peripheral rim of decreased signal intensity due to hemosiderin deposition in the surrounding parenchyma caused by repeated microhemorrhages [5, 18]. These type CA lesions are also called, as “mulberry” or “popcorn” appearance [7, 16]. CA lesions comprise deoxyhemoglobin or hemosiderin, which create magnetic susceptibility effects and cause a decrease in signal intensity [19]. These signal intensity abnormalities are better evaluated by T2*-weighted GRE sequence than by spin echo and fast spin echo images [10]. Until recently, T2*-weighted GRE sequence admitted as the most sensitive sequence in the evaluation the number of CA lesions in patients with familial forms of the disease [7, 10]. SWI is a technique that three-dimensional, high-spatial resolution, GRE MRI sequence which utilizes the magnetic susceptibility differences of various tissues or substances, such as blood products, iron, and calcification [20, 21]. Consequently, SWI is highly susceptible to the venous vasculature, blood products, and vascular malformations. Some studies have suggested that SWI is more sensitive than T2*-weighted GRE imaging for evaluating CA [4, 5, 11]. Our findings confirmed that SWI is more sensitive for detecting CAs than T2*-weighted GRE sequences. The difference in the number of lesions detected by SWI and

Value of SWI in cerebral cavernous angiomas

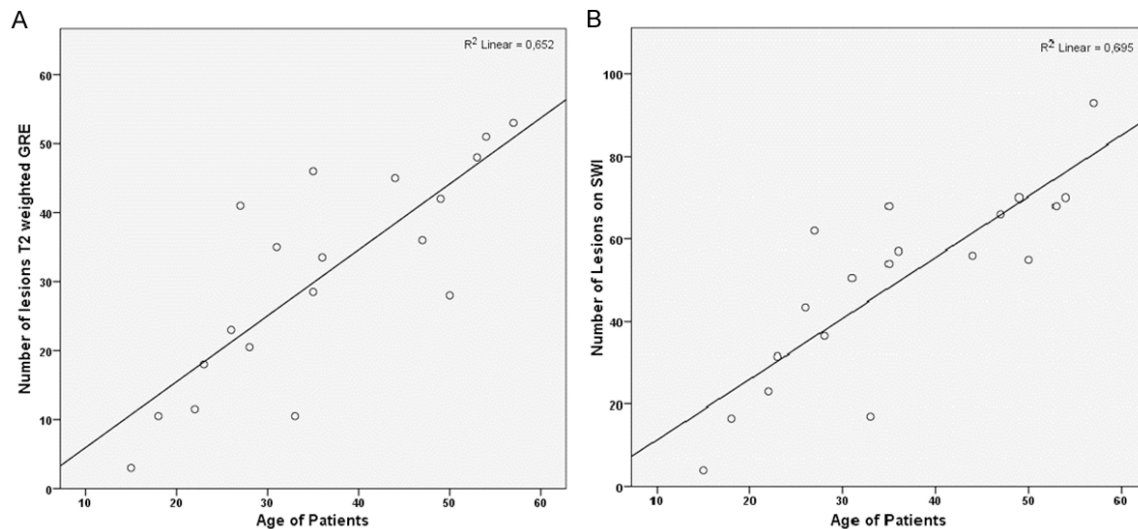


Figure 3. Correlation between age and number of lesion in familial cavernous angiomas. A. The x axis shows the age of the patients and the y axis shows the number of lesions seen on T2*-weighted GRE. B. The x axis shows the age of the patients and the y axis shows the number of lesions seen on susceptibility-weighted imaging (SWI). Age of the patients and number of CAs are well correlated for both sequences respectively. ($r = 0.81$, $P < .001$ and $r = 0.85$, $P < .001$).

T2*-weighted GRE was statistically significant in patients with familial CA ($P < 0.001$). Results of those previous studies and the study presented here suggested that SWI is more sensitive than T2*-weighted GRE imaging for detecting the number of lesions in patients with CA. The reason for this as De Souza et al. [11] proposed that the bloom effect which is marked on T2*-weighted GRE sequences and is less evident on SWI may obscure the small CA lesions and SWI is a volumetric three-dimensional, high-spatial resolution sequence with fewer artifacts related to the bone-brain interface, which may be responsible for the superiority of this sequence.

Zabramski et al. [7] have proposed a classification system ranging from types I to IV for cerebral CAs based on MRI features on conventional spin-echo and gradient echo sequences. Type I lesions are characterized by hyperintense core on T1 and hyper- or hypointensity core on T2-weighted sequences which is consistent with subacute hemorrhage. Type II lesions are characterized by a core with reticulated mixed signal intensity on T2-weighted sequences and on T1-weighted images, with a well-circumscribed hypointense rim on T2-weighted sequences which is consistent with hemorrhages and thromboses of varying ages. Type III lesions show a iso- or hypointensity on

T1-weighted sequence and a hypointensity on T2-weighted sequence as well as a rim that is hypointense on T2-weighted sequences which is consistent with chronic resolved hemorrhage or hemosiderin within and around the lesion. Type IV malformations are punctate hypointense lesions on T2*-weighted GRE MRI which is consistent with telangiectasias or in an early stage CA [7, 8, 21]. Type IV lesions show a close relationship with the familial form of CA [4, 7, 8, 11]. In this study, approximately 44% of the CA lesions detected by SWI in patients with familial CAs were not seen on T2*-weighted GRE sequences. This study show that the Zabramski classification is insufficient to identify all CA lesions, and a new type should be defined to represent lesions that are seen on SWI but not on T2*-weighted GRE. Hence, we propose a new type (type V) should be added to Zabramski classification.

The characteristics of familial form of the disease are presence of multiple lesions and development of new lesions during lifetime [3, 8, 22]. Because of complications from the familial form of CA, these patients should be included in screening surveillance programs. Also, MRI screening of family members may facilitate earlier diagnosis and better support [11]. Moreover, in patients with medically intractable or cryptogenic epilepsy and atypical

intracerebral hemorrhage, SWI can also help to confirm the diagnosis of CA in cases in which the lesion could not be detected on conventional MRI [5]. The results of present study suggest that SWI should be added in routine clinical neuroimaging protocols to assess the real prevalence of lesions for true diagnosis and treatment.

Our study had some limitations. First, due to familial CA is infrequent entity, our cohort included a limited number of patients. Second, all the with marked hypointense focuses on T2*-weighted GRE and SWI were considered as CA lesions. We have histological data from two of these lesions but some of others may have been due to calcification or bleeding from other etiologies [4, 11]. Such hypointense signals could also be observed in hypertensive angiopathy, amyloid angiopathy, hemorrhagic metastasis, vasculitis of the central nervous system, hemorrhagic diffuse axonal injury, radiation-induced telangiectasias, or even tiny lesions of fat or pneumocephalus [4, 5, 13]. Nonetheless, we also carefully investigated the clinical history of all patients and reviewed previous imaging studies to exclude additional neurological abnormalities. In addition, the low mean age of our patients excluded the possibility of other neurological abnormalities. Further studies on pathological correlations would clarify whether the lesions seen on SWI represent capillary telangiectasias or CA in an early stage.

In conclusion, SWI can provide helpful additional information by determining the CA lesions more accurately than T2*-weighted GRE. Hence, SWI should be added in routine clinical neuroimaging protocols to assess the real prevalence of lesions for true diagnosis and treatment. Moreover, this study show that the Zabramski classification is insufficient to identify all CA lesions to represent lesions that are seen on SWI but not on T2*-weighted GRE, and a new type (type V) should be added to Zabramski classification.

Disclosure of conflict of interest

None.

Address correspondence to: Dr. Haci Taner Bulut, Department of Radiology, Medical Faculty of Adiyaman University, Adiyaman, Turkey. Tel: +90

530 207 15 17; Fax: +90 416 227 08 63; E-mail: taner.bulut02@gmail.com

References

- [1] Barrow DL. Classification and natural history of cerebral vascular malformations: arteriovenous, cavernous, and venous. *J Stroke Cerebrovasc Dis* 1997; 6: 264-7.
- [2] Rigamonti D, Hadley MN, Drayer BP, Johnson PC, Hoenig-Rigamonti K, Knight JT, Spetzler RF. Cerebral cavernous malformations. Incidence and familial occurrence. *N Engl J Med* 1988; 319: 343-7.
- [3] Moriarity JL, Wetzel M, Clatterbuck RE, Javedan S, Sheppard JM, Hoenig-Rigamonti K, Crone NE, Breiter SN, Lee RR, Rigamonti D. The natural history of cavernous malformations: a prospective study of 68 patients. *Neurosurgery* 1999; 44: 1166-71; discussion 72-3.
- [4] de Champfleury NM, Langlois C, Ankenbrandt WJ, Le Bars E, Leroy MA, Duffau H, Bonafé A, Jaffe J, Awad IA, Labauge P. Magnetic resonance imaging evaluation of cerebral cavernous malformations with susceptibility-weighted imaging. *Neurosurgery* 2011; 68: 641-7; discussion 7-8.
- [5] Campbell PG, Jabbar P, Yadla S, Awad IA. Emerging clinical imaging techniques for cerebral cavernous malformations: a systematic review. *Neurosurg Focus* 2010; 29: E6.
- [6] Cortes Vela JJ, Concepcion Aramendia L, Balenilla Marco F, Gallego Leon JI, Gonzalez-Spinola San Gil J. Cerebral cavernous malformations: spectrum of neuroradiological findings. *Radiologia* 2012; 54: 401-9.
- [7] Zabramski JM, Wascher TM, Spetzler RF, Johnson B, Golfinos J, Drayer BP, Brown B, Rigamonti D, Brown G. The natural history of familial cavernous malformations: results of an ongoing study. *J Neurosurg* 1994; 80: 422-32.
- [8] Brunereau L, Labauge P, Tournier-Lasserre E, Laberge S, Levy C, Houtteville JP. Familial form of intracranial cavernous angioma: MR imaging findings in 51 families. *French Society of Neurosurgery. Radiology* 2000; 214: 209-16.
- [9] Kwon CS, Sheth SA, Walcott BP, Neal J, Eskandar EN, Ogilvy CS. Long-term seizure outcomes following resection of supratentorial cavernous malformations. *Clin Neurol Neurosurg* 2013; 115: 2377-81.
- [10] Lehnhardt FG, von Smekal U, Ruckriem B, Stenzel W, Neveling M, Heiss WD, Jacobs AH. Value of gradient-echo magnetic resonance imaging in the diagnosis of familial cerebral cavernous malformation. *Arch Neurol* 2005; 62: 653-8.
- [11] de Souza JM, Domingues RC, Cruz LC Jr, Domingues FS, Iasbeck T, Gasparetto EL. Sus-

Value of SWI in cerebral cavernous angiomas

- ceptibility-weighted imaging for the evaluation of patients with familial cerebral cavernous malformations: a comparison with t2-weighted fast spin-echo and gradient-echo sequences. *AJNR Am J Neuroradiol* 2008; 29: 154-8.
- [12] Haacke EM, Xu Y, Cheng YC, Reichenbach JR. Susceptibility weighted imaging (SWI). *Magn Reson Med* 2004; 52: 612-8.
- [13] Tsui YK, Tsai FY, Hasso AN, Greensite F, Nguyen BV. Susceptibility-weighted imaging for differential diagnosis of cerebral vascular pathology: a pictorial review. *J Neurol Sci* 2009; 287: 7-16.
- [14] Shrout PE, Fleiss JL. Intraclass correlations: uses in assessing rater reliability. *Psychol Bull* 1979; 86: 420-8.
- [15] Landis JR, Koch GG. The measurement of observer agreement for categorical data. *Biometrics* 1977; 33: 159-74.
- [16] Hegde AN, Mohan S, Lim CC. CNS cavernous haemangioma: "popcorn" in the brain and spinal cord. *Clin Radiol* 2012; 67: 380-8.
- [17] Rigamonti D, Johnson PC, Spetzler RF, Hadley MN, Drayer BP. Cavernous malformations and capillary telangiectasia: a spectrum within a single pathological entity. *Neurosurgery* 1991; 28: 60-4.
- [18] Rivera PP, Willinsky RA, Porter PJ. Intracranial cavernous malformations. *Neuroimaging Clin N Am* 2003; 13: 27-40.
- [19] Abduljalil AM, Robitaille PM. Macroscopic susceptibility in ultra high field MRI. *J Comput Assist Tomogr* 1999; 23: 832-41.
- [20] Sehgal V, Delproposito Z, Haacke EM, Tong KA, Wycliffe N, Kido DK, Xu Y, Neelavalli J, Haddad D, Reichenbach JR. Clinical applications of neuroimaging with susceptibility-weighted imaging. *J Magn Reson Imaging* 2005; 22: 439-50.
- [21] Lee BC, Vo KD, Kido DK, Mukherjee P, Reichenbach J, Lin W, Yoon MS, Haacke M. MR high-resolution blood oxygenation level-dependent venography of occult (low-flow) vascular lesions. *AJNR Am J Neuroradiol* 1999; 20: 1239-42.
- [22] Labauge P, Brunereau L, Levy C, Laberge S, Houtteville JP. The natural history of familial cerebral cavernomas: a retrospective MRI study of 40 patients. *Neuroradiology* 2000; 42: 327-32.